IMPERIAL COLLEGE LONDON

Department of Earth Science and Engineering

Centre for Petroleum Studies

Productivity of Gas Condensate Fields Below The Dew Point: A North Sea Case Study

By

Phil Lloyd

A report submitted in partial fulfilment of the requirements for the MSc and/or the DIC.

September 2011

DECLARATION OF OWN WORK

I declare that this thesis

"Productivity of Gas Condensate Fields Below The Dew Point: A North Sea Case Study"

is entirely my own work and that where any material could be construed as the work of others, it is fully cited and referenced, and/or with appropriate acknowledgement given.

Signature: ....

Name of Student: Phil Lloyd

Name of Supervisor(s): Christophe Soyeur, Total E&P UK Ltd
Alain C. Gringarten, Imperial College

ACKNOWLEDGEMENTS

I would like to thank Total E&P UK Ltd for their great support during this MSc course. The technical assistance during this project and the financial support during the year are most appreciated.

In particular, I would like to thank Christophe Soyeur for his guidance throughout the project, both with the technical work and also with giving direction for how the project should progress.

I would also like to thank Alain Gringarten of Imperial College for guidance with the structure of the project report.

TABLE OF CONTENTS

LIST OF FIGURES

LIST OF TABLES

Productivity of Gas Condensate Fields Below The Dew Point: A North Sea Case Study

P.D.W. Lloyd

Imperial College supervisor: A.C.Gringarten

Company supervisor: C.Soyeur, Total E&P UK Ltd

Abstract

This paper presents the results of combining field data from two North Sea HPHT rich gas condensate fields with a fine-gridded compositional simulation to determine the impact that producing below the dew point will have on future well productivity. The analysis here shows that the well productivity decreased when the reservoir pressure dropped below dew point due to the accumulation of condensate around the wellbore. Furthermore, the productivity index observed today, in the absence of any wellbore dry scale, should not decrease any further. The project supports the operator in the prediction of productivity evolution, corresponding to the de-risking of several million barrels of oil equivalent (boe).

Individual well multi-rate flow tests performed while the reservoir was above the dew point were analysed to determine the rate-dependent wellbore skin. A range of correlations were used to predict the evolution of this rate-dependent skin as the reservoir pressure dropped below dew point.

A phenomenological model was used to capture most of the physics associated with two-phase flow around the wellbore. The velocity dependent relative permeability phenomenon was simulated and a range of parameters investigated to create a set of realistic matches for the observed field measurements.

Introduction

Reservoir A in the North Sea is an HPHT gas condensate field with a producing GOR of 1000 Sm^3/Sm^3 and a reservoir thickness of approximately 300 m. The expectation was for well productivity to decrease significantly once the reservoir pressure dropped below dew point.

Well productivity was regularly monitored and when reservoir pressure dropped below dew point approximately two years ago, no significant impact on well productivity was observed.

The objective of this study is to review the field data and to quantify the productivity index (PI) evolution over the life of the reservoir. Measured field data was benchmarked against phenomenological model answer and used to forecast future well behaviour. This model can now be used to support the operator in predicting the expected PI evolution in the future.

At present, the full field reservoir model used by the operator to assess field reserves includes an allowance for productivity reduction due to condensate deposition in the reservoir. Full field coarse models fail to capture the condensate build-up around the well and are therefore expected to be optimistic models. Current practice is to tune the full field model to match field data by adding an extra skin to the well to represent the productivity decrease due to condensate accumulation. The reservoir pressure dropped below the dew point approximately two years ago and the full field model was updated by matching to latest flow tests. The forecast for future productivity currently carries a lot of uncertainty, and in the absence of more accurate predictions, a large range was assigned to the productivity as the reservoir pressure continues to drop. The present uncertainty in the model is such that there is a two-fold difference between productivity in the pessimistic (1P) and optimistic (3P) models.

Concept of a Condensate Bank

The phase behaviour of gas condensate fluids in the near-wellbore region is complex. Many authors have documented the physics and evidence behind this phenomenon and an in-depth review can be found in Gringarten *et al* (2000). For an application to field data see Afidick (1994).

The presence of condensate in the formation reduces the relative permeability to gas, therefore reducing well productivity. When gas condensate flows towards a well and the pressure drops below dew point, a small volume of liquid is deposited in the formation. The concentration of liquid is a function of the pressure, temperature, fluid composition and petrophysical properties of the rock. Initially, this liquid saturation is small and most likely below the critical saturation, therefore immobile. When more gas flows towards the well, more liquid is deposited, increasing the liquid saturation until eventually the critical saturation is exceeded and some condensate flows to the well. The relative permeability to condensate increases with liquid saturation until eventually a dynamic equilibrium is formed between the liquid condensing from the gas and the flow of liquid from the "condensate bank" towards the well. An extension to this description is required because it was observed experimentally by Boom *et al* (1995) that condensate saturation in the near-well region reduces with increasing capillary number, N_c:

$$\boldsymbol{N_c} = \frac{\boldsymbol{v_g \mu_g}}{\boldsymbol{\sigma}} \quad \text{......} \quad (1)$$

where N_c = capillary number, v_g = gas velocity, μ_g = gas viscosity and σ = interfacial tension between gas and condensate.

Calculating Well Productivity for Single Phase Flow

The semi steady state inflow equation (Eq. 2) is used to represent single phase radial flow

$$m(p)_{res} - m(p)_{bh} = \frac{1422\, Q\, T}{k_e h}\left(ln\frac{r_e}{r_w} - \frac{3}{4} + S\right) \quad \text{......} \quad (2)$$

where *m(p)* is the gas pseudo-pressure as defined by Al Hussainy (1966) (Eq. 3) for the reservoir (*res*) and the bottom hole (*bh*), *Q* is the standard gas flow rate, *T* is the absolute temperature, k_e is the effective permeability, *h* is the reservoir thickness, r_e is the equivalent drainage radius, r_w is the well radius and *S* is the total apparent wellbore skin. All values are in field units.

$$m(p) = 2\int_{p_{ref}}^{p} \frac{p}{\mu(p)z(p)}dp \quad \text{......} \quad (3)$$

The productivity index, defined as the flow rate divided by the drawdown, can then be calculated. For this study, the wellbore skin is the parameter used to monitor well productivity. The components of total skin can be represented by Eq. 4, where *D* is the so-called "D-Factor", defined by Swift (1962):

$$S_{Total} = S_{mechanical} + D\, Q \quad \text{......} \quad (4)$$

Eq. 4 substituted into Eq 2 rearranges to:

$$\frac{m(p)_{res} - m(p)_{bh}}{Q} = \frac{1422\, T}{kh}\left(ln\frac{r_e}{r_w} - \frac{3}{4} + S_{mechanical}\right) + \frac{1422\, T}{kh} D\, Q \quad \text{......} \quad (5)$$

Therefore a plot of *[m(p)*$_{res}$ – *m(p)*$_{bh}$*] / Q* vs *Q* will give a slope of *1422 T D / kh*, from which the D-Factor can be calculated.

Non-Darcy Flow

Throughout the majority of the reservoir, flow rates are low and pressure drop is proportional to flow rate (Darcy's Law). Forchheimer (1901) observed that at sufficiently high rates, the observed pressure drop is higher than that predicted by Darcy's Law and is a function of the gas rate. This can be described by the Forchheimer equation (Eq. 6):

$$\frac{dp}{dx} = \left(\frac{\mu}{k_e}\right)v + \beta\,\rho\, v^2 \quad \text{......} \quad (6)$$

where *dp/dx* is the pressure gradient, β is the inertial flow coefficient, *v* is the gas velocity and ρ is the gas density.

Many correlations exist for β, in the form shown in Eq. 7, each with different values for the effective porosity exponent (*c*) and effective permeability exponent (*d*). The gas saturation (S_g) is included to create an effective porosity term ($\varphi\ S_g$). These relationships assume that the liquid phase is immobile.

$$\beta \propto \left(\varphi S_g\right)^c . k_e^d \quad \text{......} \quad (7)$$

D-Factor Evolution

The D-Factor introduced in Eq. 4 is defined according to Swift (1962):

$$\boldsymbol{D} = \frac{\boldsymbol{2.715\, x\, 10^{-15}\, \beta\, M\, p_{sc} k_e}}{\boldsymbol{\mu\, h\, r_w\, T_{sc}}} \quad \text{......} \quad (8)$$

where p_{sc} and T_{sc} are pressure and temperature at standard conditions, and *M* is the gas molecular weight, all in field units.

Gas viscosity is a function of pressure. For a reservoir with high initial pressure, such as the one considered in this study, the viscosity change over the life of the reservoir will be significant. Therefore, according to Eq. 8, the D-Factor will also change over time. Furthermore, below the dew point, effective permeability and effective porosity both decrease as liquid saturation in the reservoir builds up, so the value of β, determined from correlations in the form shown in Eq. 7, will also change.

Work performed by Gringarten *et al.* (2011) focused on the assessment of a D-Factor at a particular point in time with a fixed reservoir pressure. The gas viscosity will therefore be reasonably constant at that particular pressure. This study focuses not on the determination of a D-Factor, but on how this value can be used to predict future well and reservoir performance. With depletion, the reservoir pressure and the viscosity will change; therefore the D-Factor calculated at a particular reservoir pressure will evolve with reservoir pressure according to Eq. 8.

Velocity Dependent Relative Permeability

Henderson *et al* (2000) described mathematically (Eq. 9, 10, 11, 12) the effect that the capillary number has on condensate saturation and relative permeability. It was observed that these effects only occurred above a base capillary number (N_{cb}). As the capillary number increases, the relative permeability curves increase from their base curves towards straight "miscible" curves (Figure 1), according to:

$$k_r = Y\,k_{rb} + (1-Y)k_{rm} \quad (9)$$

where Y is the scaling function,

$$Y = \left(\frac{N_{cb}}{N_c}\right)^n \quad (10)$$

The straight miscible relative permeability curves are described as:

$$k_r = \left(\frac{S^*-S_r}{1-S_r}\right) \quad (11)$$

where S^* is the condensate saturation relative to hydrocarbon pore volume, $S^* = S\,/\,(1 - S_w)$, and the residual condensate saturation varies with parameter "m" according to:

$$S_r = (1-e^{-mY})\,S_{rb} \quad (12)$$

This velocity dependent relative permeability model was used in the phenomenological model described later, in order to represent the expected reduction in liquid saturation and relative permeability very close to the wellbore.

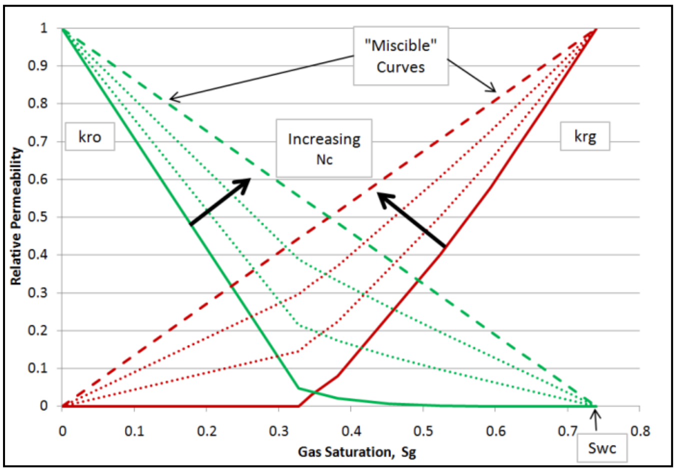

Figure 1: Effect of Velocity Dependent Relative Permeability Parameters on Relative Permeability Curves

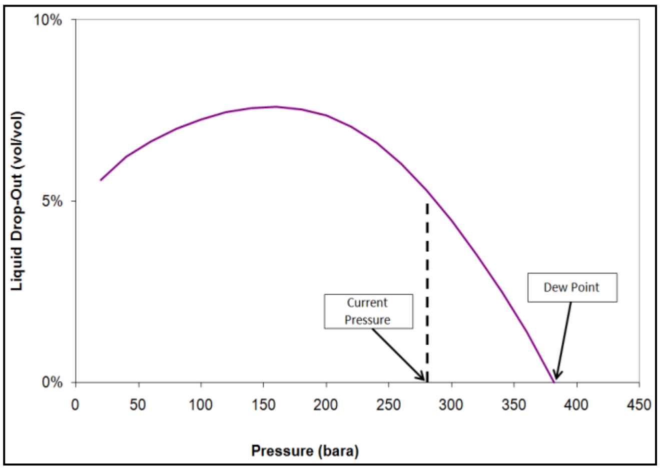

Figure 2: CVD Liquid Drop-Out Curve for Reservoir A Fluids

Reservoir Overview

Reservoir A is Upper Jurassic sandstone with thickness 300 m, temperature 190°C, and initial pressure 1150 bara. Well A1 is a sub-vertical high-rate producer with initial gas flow rate 3 MSm^3/d down to current rate of 1.1 MSm^3/d. The reservoir contains supercritical fluid with GOR 1000 Sm3/Sm3 and dew point 382 bara. Figure 2 shows the Constant Volume Depletion (CVD) liquid drop-out curve. Average permeability of 18 mD and porosity 17% are observed.

Part 1: Field Observations

In order to assess observed well productivity variation below dew point, flow test data was used to calculate wellbore skin. High temperatures mean that downhole pressure meters have a short lifespan and the available downhole pressure build-up data is limited. Vapour and condensate flow rates were inferred by difference by measuring the total field production rate at the slug catcher then measuring the stabilised rate after the subject well was shut-in. A back-pressure correction was then applied to the flow rates to account for the resulting increased production from other wells. For each well production test, tubing head pressures (THP) were recorded at the wellhead and flowing bottomhole pressures (BHP) calculated from the THP using the OLGA 2P flow correlation and the Peng-Robinson compositional PVT model, using the standard gas and condensate flow rates measured in the flow test. The commercial software *PROSPER* was used for the BHP calculations. Static reservoir pressures were taken from the full-field model in order to calculate a drawdown.

This analysis was performed on several wells in Reservoir A. The well showing the least scattered data was selected as the candidate well for numerical well modelling.

Production Rate and GOR

The gas production rate and GOR history of Well A1 is shown in Figure 3. Each measurement was made by flow test with a fully open choke. The GOR shows a constant value above the dew point, and then increases steadily below the dew point, showing that condensate is left in the formation and leaner gas produced. The effect of velocity stripping is not seen in the GOR evolution because the near-well volume affected by this phenomenon is very small compared to the volume of the reservoir. The gas rate declines steadily over time, increasing step-wise after each acid wash.

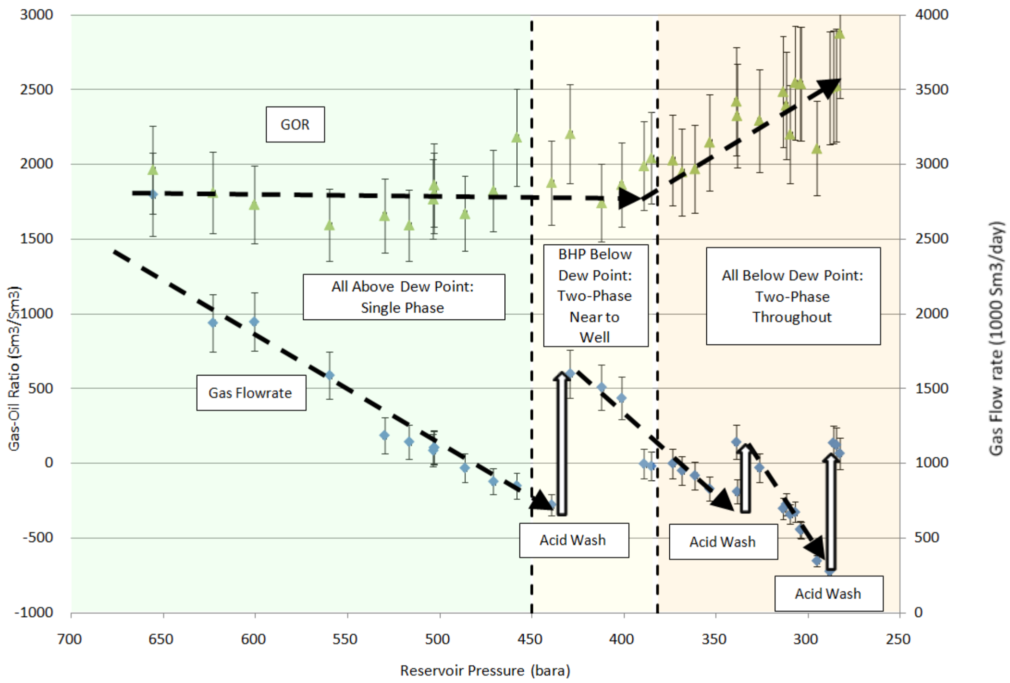

Figure 3: Gas Production Rate and GOR vs Reservoir Pressure for Well A1

Skin Evolution

Total wellbore skin was calculated for each flow test using Eq. 2, with r_w = 0.11 m and r_e = 1250 m. The skin evolution is shown in Figure 4. The drawdown between reservoir and wellbore causes condensate to drop out in the near-well formation while the reservoir pressure is above dew point. The approximate region where BHP drops below dew point is shown.

The build-up of dry scale around the wellbore is significant and causes the high skin values observed in Figure 4. It was confirmed by operations that the scale is anhydrous $CaCO_3$ rather than any wet scale caused by the production of formation water. The acid washes were performed to dissolve this dry scale and to reduce the wellbore skin.

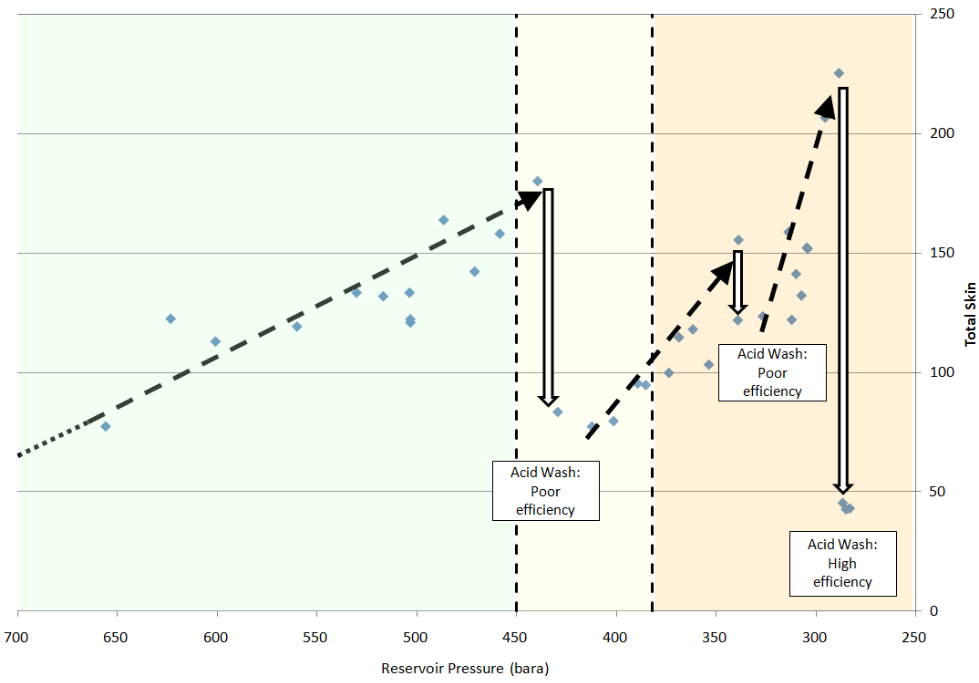

Figure 4: Total Skin vs Reservoir Pressure for Well A1

Measurement of D-Factor Above Dew Point

Eq. 5 shows how single phase multi-rate tests can be used to measure a D-Factor for rate-dependent skin estimation. Flow tests from Well A1 were made at similar rates so multi-rate analysis was not possible. Instead, analysis was performed on flow tests from nearby Well B2 in Reservoir B where flow tests at different rates were performed on the same day. Reservoir B is also an HPHT gas condensate field with richer gas to Reservoir A. The permeability of Reservoir B is an order of magnitude higher.

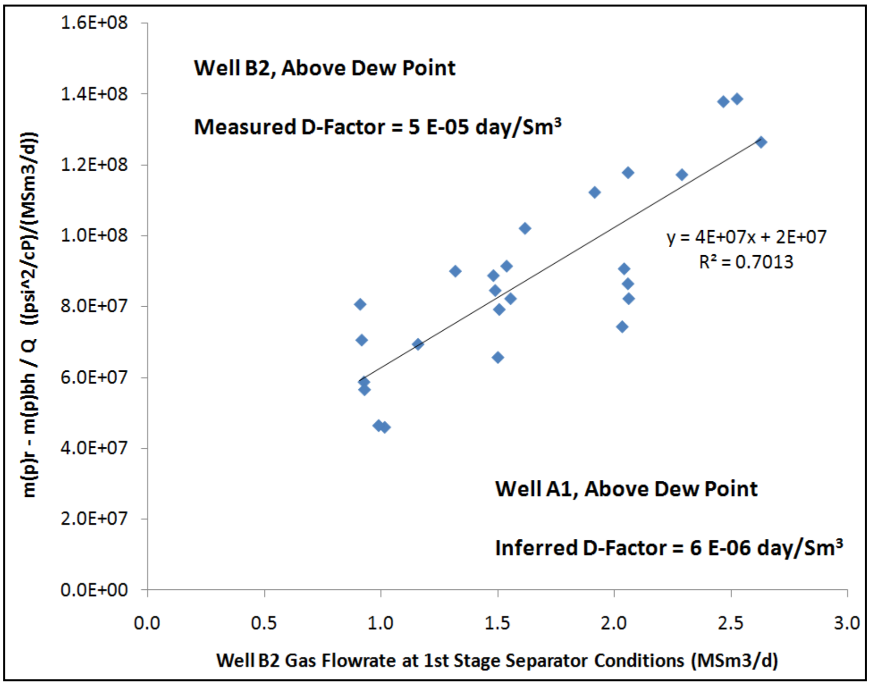

Twenty six multi-rate flow tests between reservoir pressures of 780 bara and 550 bara were analysed and the results plotted together in Figure 5. The best-fit line for these plots yields an average single-phase D-Factor for Well B2 at an average reservoir pressure of 650 bara of 5 x 10^{-5} day/Sm3. The relationship between D-Factor and the permeability, viscosity and specific gravity, shown in Eq. 6, was used to scale this result to estimate a single-phase D-Factor for Well A1 at 650 bara of approximately 6 x 10^{-6} day/Sm^3.

Figure 5: Multi-Rate Flow Test Analysis for Well B2 to Determine Single-Phase D-Factor at Reservoir Pressure of 650 bara

Comments on Field Observations

- Evolution of total skin is mainly dominated by dry scaling.
- The lowest recorded total skin was in the last three flow tests when reservoir pressure was below dew point.
- The increasing GOR trend below dew point confirms that condensate remains in the formation.

- Well A1 has been acidized three times. A different operational method was deployed during the last acid job allowing better treatment efficiency.
- D-Factor calculations from Well B2 were used to estimate a D-Factor for Well A1,.
- No data available for the three years of production prior to 2004.

Uncertainties in Field Observations

Measurements of the flow rate and the computation of the corresponding drawdown are subject to a certain level of uncertainty. Flow rates are typically accurate to 10% but other factors add to this uncertainty. The flow rates are measured by difference so the accuracy of the applied back-pressure correction strongly affects the derived flow rate. If no back-pressure correction is applied then rates are under-predicted.

The BHP estimation requires accurate fluid characterisation and gas and condensate flow rates. A small error in BHP or reservoir pressure will result in a large error in drawdown, and therefore in the skin calculation.

Conclusion from Field Observations

- It appears that the impact of condensate accumulation in the wellbore has a minor impact, if any, when compared with the impact of dry scaling.
- Good sustained well productivity has been confirmed below dew point.
- No PI reduction associated with reservoir pressure dropping below dew point can be identified with the available data set.

Part 2: Well Productivity Evolution Modelling

The results from Part 1 were compared with phenomenological well model answers in order to find the model which best fits the field observations.

A fine-grid single-well radial compositional simulation model was used to capture most of the physics associated with two-phase flow around the wellbore. A model was constructed using commercial software *ECLIPSE300*. The radial model comprised 22 log radial cells with high cell density in the few meters around the wellbore to capture the fluid behaviour where the pressure gradient is highest. Average reservoir properties encountered at Well A1 were used in the model. Both rate-dependent non-Darcy effects and velocity dependent relative permeability effects were represented in the model.

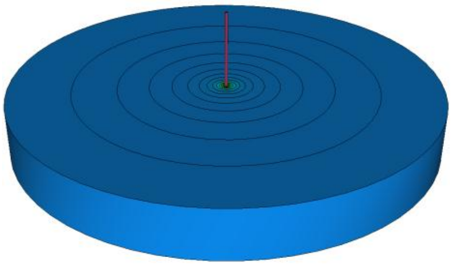

Figure 6: Phenomenological Well Model of Reservoir A

Table 1: Well A1 Fine-Grid Model Construction

Parameter	Value
Well Radius	0.11 m
Inner/Outer Cell Radius	0.25 m – 1235 m
Cell Count	22
Formation Thickness	297 m
Net-to-Gross Ratio	0.86
Average Porosity	17%
Average Permeability	18 mD
kv / kh	0.2

Model Parameters

The model was tuned in three ways, by adjusting: the inertial flow coefficient (β), both its absolute value and rate of increase with depletion; the velocity dependent relative permeability; and the permanent mechanical skin. No attempt was made to model the build up of dry scale because this effect is independent of fluid effects and was not the purpose of this modelling exercise. The intention of the modelling was to ascertain the effect that liquid accumulation and changing fluid properties have on the future well productivity.

Model Analysis

The reservoir model does not give access to a total skin as described in Part 1, so the simulated skin evolution was calculated separately using Eq. 2. Both the velocity stripping and D-Factor functionality were activated in the model. The model was tuned to match the observed skin by varying a set of parameters within limits derived for this field by Barker (2005). The range of values used for the velocity dependent relative permeability and D-Factor evolution are shown in Table 2.

Table 2: Range of Values for Velocity Dependent Relative Permeability and Inertial Flow Coefficient (β) Evolution

Function	Parameter	Description	Min	Mid	Max
VDRP	N_{cb}	Base capillary number	2×10^{-7}	2×10^{-6}	2×10^{-5}
VDRP	m_g	Critical saturation modifier, gas	4	20	40
VDRP	n_c	Weighting factor for capillary number ratio	33	67	100
β	c	Effective porosity exponent	-0.31	-0.21	-0.11
β	d	Effective permeability exponent	-2.65	-2.15	-1.15

Two Phase Fluid Behaviour Below Dew Point

A simulation was performed without any imposed velocity- or rate-dependent conditions, to identify the basic model behaviour. Figure 7 shows the profile of condensate saturation with distance from the wellbore on a semi-log scale, for decreasing reservoir pressures. When the reservoir pressure falls below the dew point of 382 bara, condensate saturation far from the wellbore is close to zero (P_{res} = 380 bara), increasing significantly in the 10m around the wellbore to a maximum at the wellbore. The condensate saturation stabilises when equilibrium forms between the rich gas flowing in from the reservoir, and the condensate flowing out into the wellbore due to its increased mobility.

With further depletion, the size of the condensate bank expands further into the reservoir and the saturation in the reservoir increases, as predicted by liquid drop-out laboratory results. The saturation near the wellbore is lower than it was at high pressure which is a key result for well productivity. Depletion causes lower gas flow rates, which means less rich gas flows towards the wellbore and the equilibrium of high condensate saturation can no longer be sustained, therefore the near-well saturation reduces with depletion. This implies an increasing relative permeability of the dominant (gas) phase.

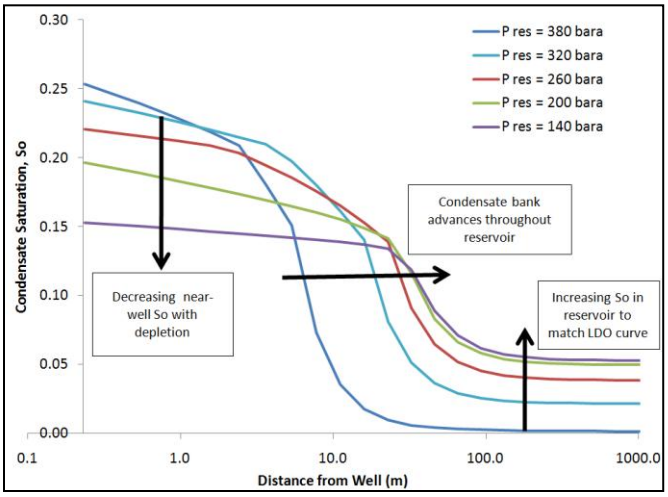

Figure 7: Condensate Saturation vs Distance from Wellbore for Decreasing Reservoir Pressure

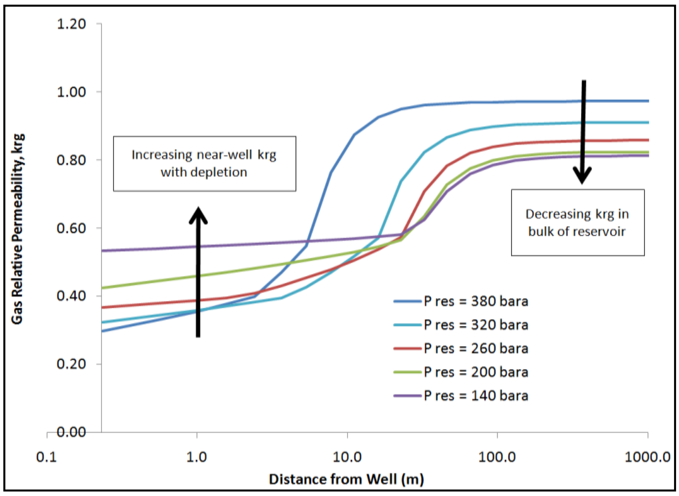

Figure 8: Gas Relative Permeability vs Distance from Wellbore for Decreasing Reservoir Pressure

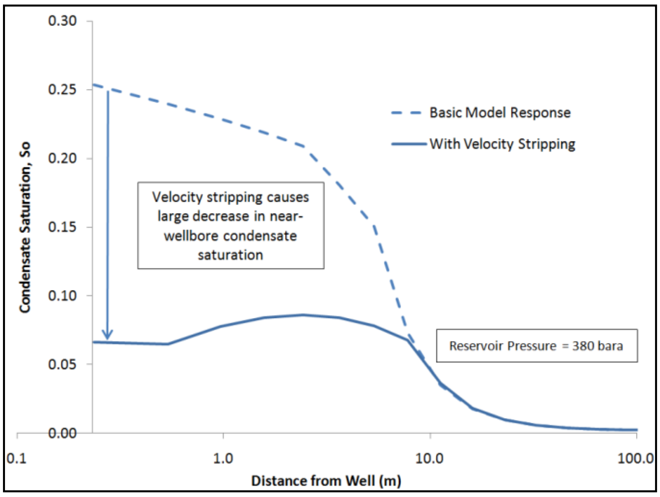

Figure 9: Typical Effect of Velocity Stripping on Condensate Saturation for Reservoir Pressure 380 bara

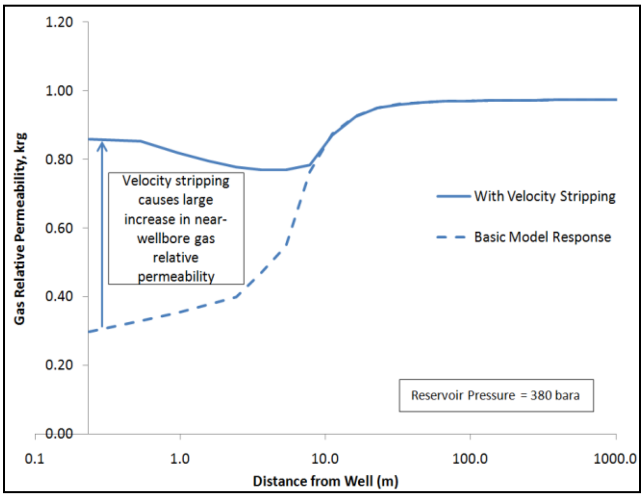

Figure 10: Typical Effect of Velocity Stripping on Gas Relative Permeability,, for Reservoir Pressure 380 bara

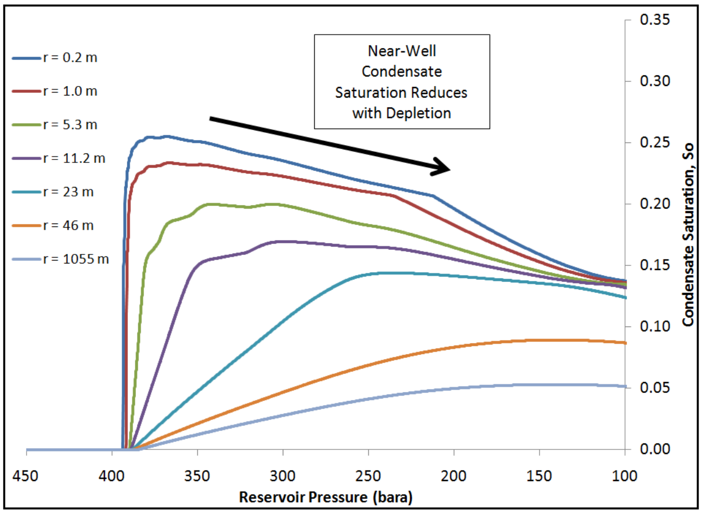

Figure 11: Condensate Saturation vs Reservoir Pressure for Increasing Distance from Wellbore

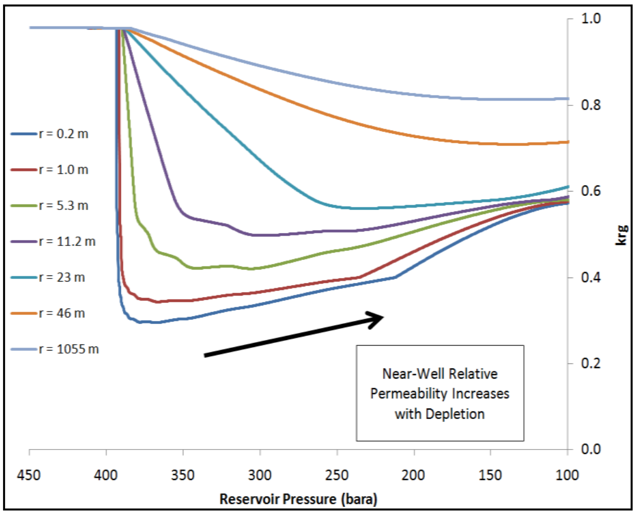

Figure 12: Gas Relative Permeability vs Reservoir Pressure for Increasing Distance from Wellbore

D-Factor Evolution Below Dew Point

Many different correlations exist for the coefficient of inertial flow resistance (β), each with different dependencies on petrophysical properties. Appendix 1 shows a range of correlations published to date, by Tek *et al* (1962), Geertsma (1974), Pascal *et al* (1980), Noman *et al* (1985), Jones (1987), Evans *et al* (1987), Coles and Hartman (1998), Barker (2005), and Aminian *et al* (2007). All of the correlations were derived from core experiments and all show reasonable consistency for the samples studied. Above the dew point, the correlations are reasonably consistent. The only variations arise from how rock compaction and its associated reduction in porosity and permeability are modelled. However, once the dew point is passed and the effective permeabilities and porosities show large changes, the correlations exhibit very different trends. What is clear from reviewing these papers is that there is no one correlation which can be used in all circumstances. Figure 13 shows the variation in the D-Factor when the correlations for β were applied to well A1. These values have all been normalised at 800 bar so the influence of variations in k, ϕ and S_o can be seen. Figure 13 shows that if the correlations are first calibrated against a multi-rate test, then the predictions of D-Factor evolution above the dew point are reasonably consistent. However, below the dew point, the way the correlations treat the changing relative permeability and effective porosity result in large variations.

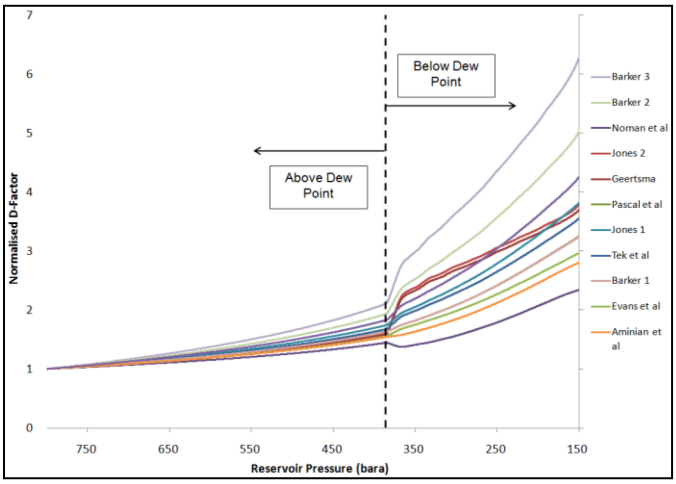

Figure 13: Variation of Normalised D-Factor with Pressure for a Variety of Published Correlations

Simulation Results and Discussion

Multiple simulations were performed to investigate the effect of capillary number, inertial flow coefficient (β) and mechanical skin on the evolution of total skin.

Figure 14 shows the results of a few selected simulations to highlight the sensitivity of the total skin evolution to these parameters. The green line (bottom) shows the model response when rate-dependent skin and velocity stripping are neglected. This is not a realistic case because these phenomena are known to occur, but is included here to show the basic trend below the dew point. Once the dew point is crossed, high condensate saturation quickly forms around the wellbore (Figure 7) with a corresponding reduction in gas relative permeability (Figure 8), causing the sharp total skin increase in Figure 14. With depletion, the condensate saturation in the near-wellbore region decreases (Figure 11) because there are lower volumes of rich gas flowing towards the wellbore, and therefore lower condensate accumulation. The gas relative permeability therefore increases gradually with depletion (Figure 12), evident by the gradual total skin decline below the dew point in Figure 14.

A mechanical skin of 10 was included in the models to represent permanent skin from the well completion. The effect of increasing mechanical skin is to simply increase all the values of total skin, as expected.

The blue line (top) includes rate-dependent skin. The magnitude of the rate-dependent skin was constrained to match the D-Factor derived from flow tests. The value of the rate-dependent skin at the control point of 650 bara was calculated by

$S_{rate\text{-}dependent} = D\,Q$, using $D = 6 \times 10^{-6}$ day/Sm^3 and $Q = 2$ MSm^3/d, giving a rate-dependent skin of approximately 12. Within the limits sets out in Table 2, the D-Factor increases most rapidly below dew point using the relative permeability exponent (d) of -2.65. The blue line (top) represents both the increase in skin due to condensate blockage around the wellbore and also the increased magnitude of the rate-dependent skin, caused by the large jump in D-Factor shown in Figure 13. As the pressure drops further, the decreasing flow rate serves to reduce the rate-dependent skin, and the total skin reduces further for the same reasons as the green line (bottom).

The red line (middle) includes the same D-Factor evolution as the blue line (top) but also includes the velocity stripping term which serves to reduce the condensate saturation around the wellbore for high gas velocities (Figure 9). The base

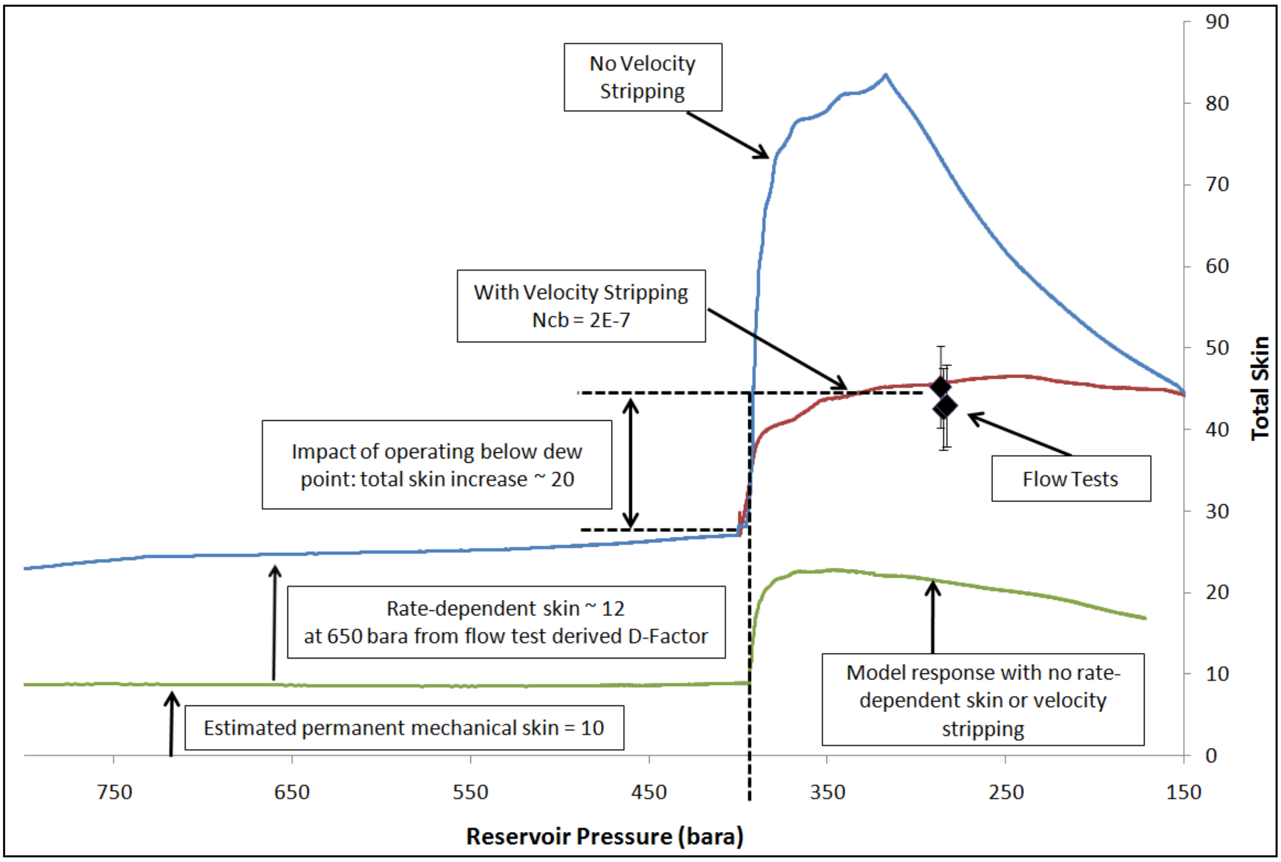

Figure 14: Range of Skin Evolution Trends

capillary number chosen was the minimum value within the range in Table 2 ($N_{cb} = 2 \times 10^{-7}$) which gives the biggest reduction in skin. The effect of this phenomenon is to significantly decrease the peak, resulting in a small increase at the dew point followed by a gradual skin increase over approximately 100 bar. It is estimated that the impact of operating below the dew point has increased the total skin by approximately 20.

What can be seen from all of the cases is that at the current reservoir pressure of 280 bara, no further increase in total wellbore skin is expected. In the most pessimistic case, the red line (middle) describes the reservoir behaviour and predicts no further change in wellbore skin or well productivity. A more optimistic case would be if the rate-dependent skin was over-predicted from the multi-rate flow tests, and/or if the permanent mechanical skin was over-predicted. Combined with a level of velocity stripping less than shown in the red line (middle), the model can fit the flow test data and will show a decrease in total skin from this point forward.

This demonstration that the skin will either remain constant at its current level, or decrease, enables a significant amount of reserves to be de-risked. Initial estimates indicate that several million boe can be added to the reserves.

Conclusions

1. The project supports the operator in the prediction of productivity evolution. No further reduction of productivity index is predicted, corresponding to the de-risking of several million boe.
2. The effect on the productivity of Well A1 from operating below the dew point was less than originally expected, and very small in comparison to the reduction in productivity caused by dry scaling.

3. Due to limitations in the historical data recovered and due to the uncertainties associated with flow test measurement, the quantification of the total skin increase, and therefore the productivity index reduction, is difficult to accurately predict.

Recommendations

1. The benefit of these results can be realised through the generation of a coarse grid model to match the fine grid radial model presented here. By applying a skin to the wellbore, the effect of observed condensate accumulation can be represented in the coarse model. It is recommended that the next step is to match this range of results using a coarse model and then implement into a full-field model to quantify the increase in reserves estimation.

Nomenclature

BHP	Bottom Hole Pressure
boe	Barrels of Oil Equivalent
c	Effective Porosity Exponent
CVD	Constant Volume Depletion
d	Effective Permeability Exponent
D	Non-Darcy Coefficient
dP / dx	Pressure Gradient
GOR	Gas-Oil Ratio
h	Reservoir Thickness
HCPV	Hydrocarbon Pore Volume
HPHT	High Pressure, High Temperature
k	Permeability
k_r	Relative Permeability
k_e	Effective Permeability (= $k * k_r$)
M	Molecular Weight
m_g	Critical saturation modifier, gas
kv / kh	Vertical / Horizontal Permeability Ratio
m(p)	Single Phase Pseudo-Pressure
MSm^3/d	Million Standard Cubic Meters per Day
n	Capillary Number Ratio Exponent
N_c	Capillary Number
N_{cb}	Base Capillary Number
p	Pressure
PI	Productivity Index
Q	Gas Flow Rate
r_e	Effective Drainage Area
r_w	Well Radius
S	Skin
S*	Condensate Saturation Relative to HCPV
S_o	Oil / Condensate Saturation
S_{wc}	Connate Water Saturation
SCAL	Special Core Analysis
T	Temperature
THP	Tubing Head Pressure
v	Velocity
VDRP	Velocity Dependent Relative Permeability
Y	$= N_c / N_{cb}$

Greek

β	Inertial Flow Coefficient
γ	Specific Gravity
μ	Viscosity
ϕ	Porosity
ρ	Density
σ	Interfacial Tension

Subscripts

b	Base
bh	Bottom Hole
g	Gas
i	Initial
m	Miscible
ref	Reference
res	Reservoir
sc	Standard Conditions

References

1. Afidick, D., Kaczorowski, N.J., Bette, S., 1994: "Production Performance of a Retrogradfe Gas Reservoir: A Case Study of the Arun Field", Paper SPE 28749 presented at the SPE Asia Pacific Oil & Gas Conference, Melbourne, Australia, 7-10 November.
2. Aminian, K., Ameri, S., Yussefabad, A.G., 2007, "A Simple and Reliable Method for Gas Well Deliverability Determination", paper SPE 111195
3. Al-Hussainy, R., Ramey, H.J.Jr, Crawford, P.B., 1966: "The Flow of Real Gases Through Porous Media", Journal of Petroleum Technology, May 1966, presented at SPE Annual Fall Meeting, Denver, 3-6 October 1965
4. Barker, J.W., 2005: "Experience with Simulation of Condensate Banking Effects in Various Gas/Condensate Reservoirs", Paper IPTC 10382 presented at the IPTC conference held in Doha, 21-23 November
5. Boom, W., Wit, K., Schulte, A.M., Oedai S., Zeelenberg, J.P.W., Maas, J.G., 1995: "Experimental Evidence for Improved Condensate Mobility at Near-wellbore Flow Conditions", Paper SPE 30766 presented at the SPE Annual Technical Conference & Exhibition, Dallas, 22-25 October
6. Coles, M.E., Hartman, K.J., 1998: "Non-Darcy Measurements in Dry Core and the Effect of Immobile Liquid", Paper SPE 39977 presented at the SPE Gas Technology Symposium, Calgary, 15-18 March
7. ECLIPSE300 Reservoir Engineering Software, version 2009.1, Schlumberger
8. Evans, R.D, Hudson, C. S., Cheenlee, J.H, 1987"The Effect of an Immobile Liquid Saturation on the Non-Darcy Flow Coefficient in Porous Media", Paper SPE 14206 presented at the 60th Annual Technical Conference, Las Vegas, Nevada, USA, 22-25 September

9. Forchheimer, P., 1901: “Wasserbewegung durch Boden” ZVD1, (45) 1781*
10. Geertsma, J., 1974: “Estimating the Coefficient of Inertial Resistance in Fluid Flow Through Porous Media”, Paper SPE 4706
11. Gringarten, A.C., Al-Lamki, A., Daungkaew, S., Mott, R., Whittle, T.M., 2000: “Well Test Analysis in Gas-Condensate Reservoirs”, Paper SPE 62920 presented at the SPE Annual Technical Conference and Exhibition, Dallas, 1-4 October
12. Gringarten, A.C., Ogunrewo, O., Uxukbayev, G., 2011: “Assessment of Rate-Dependent Skin Factors in Gas Condensate and Volatile Oil Wells”, Paper SPE 143592 presented at the SPE EUROPEC/EAGE Annual Conference and Exhibition, Vienna, Austria, 23-26 May
13. Henderson, G.D., Danesh, A., Tehrani, D.H., Al-Kharusi, B., 2000: “The Relative Significance of Positive Coupling and Inertial Effects on Gas Condensate Relative Permeabilities at High Velocity”, Paper SPE 62933 presented at the 2000 SPE Annual Technical Conference and Exhibition, Dallas, 1-4 October
14. Jones, S.C. 1987: “Using the Inertial Coefficient, β To Charactierize Heterogeneity in Reservoir Rock”, Paper SPE 16949 presented at the 62nd Annual Technical Conference and Exhibition of the the SPE, Dallas, 27-30 September
15. Noman, R., Shrimanker, N., and Archer, J.S., 1985: “Estimation of the Coefficient of Inertial Resistance in High-Rate Gas Wells,” Paper SPE 14207 presented at the 60th Annual Technical Conference, Las Vegas, Nevada, USA, 22-25 September
16. Pascal, H., Quillian, G., Kingston, D.J., 1980: “Analysis of Vertical Fracture Length and Non-Darcy Flow Coefficient using Variable Rate Tests”, Paper SPC 9348 presented at the 55th Annual Fall Technical Conference and Exhibition of the SPE of AIME, Dallas, 21-24 September
17. PROSPER, software, version 11.5, Petroleum Experts Ltd
18. Swift, G.W., Keil, O.G., 1962: “The Prediction of Gas Well Performance Including the Effect of Non-Darcy Flow” Paper SPE 143 presented at 36th Annual Fall Meeting of SPE, Dallas, 8-11 October
19. Tek, M.R., Coats, K.H., Katz, D.L. 1962: “The Effect of Turbulence on Flow of Natural Gas Through Porous Reservoirs” paper SPE 147

APPENDIX 1

Source	Inertial Flow Coefficient Correlation	Source	Inertial Flow Coefficient Correlation
Tek *et al* (1962)	$\boldsymbol{\beta \propto \frac{1}{k^{1.25}} \cdot \frac{1}{\varphi^{0.75}}}$	Evans *et al* (1987)	$\boldsymbol{\beta \propto \frac{1}{k^{0.787}} \cdot \frac{1}{\varphi}}$
Geertsma (1974)	$\boldsymbol{\beta \propto \frac{1}{k^{0.5}} \cdot \frac{1}{\varphi^{5.5}}}$	Coles and Hartman (1998)	$\boldsymbol{\beta \propto \frac{1}{k^{1.88}} \cdot \varphi^{0.449}}$
Pascal *et al* (1980)	$\boldsymbol{\beta \propto \frac{1}{k^{1.176}}}$	Barker[1] (2005)	$\boldsymbol{\beta \propto \frac{1}{k^{1.15}} \cdot \frac{1}{\varphi^{0.11}}}$
Noman *et al* (1985)	$\boldsymbol{\beta \propto \frac{1}{k^{0.5}} \cdot \varphi^{0.5}}$	Barker[2] (2005)	$\boldsymbol{\beta \propto \frac{1}{k^{2.15}} \cdot \frac{1}{\varphi^{0.21}}}$
Jones[1] (1987)	$\boldsymbol{\beta \propto \frac{1}{k^{1.55}}}$	Barker[3] (2005)	$\boldsymbol{\beta \propto \frac{1}{k^{2.65}} \cdot \frac{1}{\varphi^{0.31}}}$
Jones[2] (1987)	$\boldsymbol{\beta \propto \frac{1}{k^{0.52}} \cdot \frac{1}{\varphi^{5.68}}}$	Aminian *et al* (2007)	$\boldsymbol{\beta \propto \frac{1}{k^{0.834}}}$

Table A1: Range of published correlations for Inertial Flow Coefficient

APPENDIX 2 – LITERATURE REVIEW

SPE 62932
Measurements and Simulation of Inertial and High Capillary Number Flow Phenomena in Gas-Condensate Relative Permeability

Authors: Robert Mott, Andrew Cable and Mike Spearing (2000)

Contribution to the understanding of gas condensate reservoirs

Quantified the effect that high velocities have on the productivity of a well.

Objective of the paper

Lab experiments have confirmed that gas condensate relative permeabilities increase at high velocity (straightening the rel perm curves), whereas inertial flow effects (non-Darcy) can reduce effective gas permeability.
This paper aims to quantify the relative magnitudes of each of these effects.

Methodology used

Relative permeability measurements on a low permeability sandstone core using a 5-component gas-condensate fluid.
Used a pseudo-steady-state technique at high pressure and high velocity to recreate near-wellbore conditions.

Conclusions reached

Most important parameter for determining condensate well productivity is the effective gas permeability in the near well region, where very high velocities can occur.
Velocity stripping and the associated increase in gas relative permeability can outweigh the negative effect of condensate banking.
Inertial flow coefficient in a 3-phase gas-condensate-water system is about 50% higher than in the equivalent 2-phase gas-water system.

SPE 28749
Production Performance of a Retrograde Gas Reservoir: A Case Study of the Arun Field

Authors: D. Afidick, N.J.Kaczorowski, S.Bette, Mobil Oil Indonesia (1994)

Contribution to the understanding of gas condensate reservoirs

Applied compositional modelling to pressure transient response of wells to predict future well performance

Methodology used

1. Well productivity plots confirmed the drop in productivity.
BHP estimated from FWHP and compositional tubing hydraulics. Reservoir pressure inferred from interpolation of static bottom hole pressures.
2. Single layer compositional model used to verify that liquid accumulation would cause the same effect observed in the field.
Effect of liquid water vaporising into the vapour phase because of the high temperatures was included in the model.
Experimentally determined relative permeability curves were not an adequate representation of the reservoir and fluid phases so gas relative permeability at critical liquid saturation was increased, forcing the model's krg to be straight.
Applicability of radial model was confirmed by creating a pressure transient test with flowing BHP above dew point and then analysing it using well test software.
Model was used to generate a drawdown response after a 3-month shut-in at a reservoir pressure below the dew point. The derivative curve showed a negative half slope, indicative of liquid accumulation around the wellbore. The derivative showed two stabilisation regions, corresponding to the kh for the condensate bank and that of the rest of reservoir. The ratio of the two kh values was equal to krg at Soc. The value of krg at maximum liquid dropout was 0.99.
3. Multi-layer compositional model used to model a specific well.

Observations

Significant drop in PI occurred when the FBHP went below dew point. This made it most likely that the negative half slope seen on the derivative curve was not due to spherical flow or multi-layer effects, but was due to liquid accumulation, the only phenomenon affected by the dew point.
The model predicted very little revaporisation of accumulated condensate when the well is shut in. This is most likely because there is very little gas migration at the shut-in well, so a new equilibrium is formed in the near-well region between the accumulated condensate and the gas.
In the multi-layer well, the condensate build-up in each layer is roughly proportional to the kh of the layer. Therefore, liquid accumulation has a normalising affect on layered systems.

Conclusions reached

Liquid accumulation confirmed in the Arun reservoir by well test interpretation and PI plots and verified with compositional simulation.
With lean gas, liquid accumulation reduced individual well PI by up to 50%
Most dominant factor is Krg at Soc
Krg at Soc was determined from well test analysis, but Soc cannot be determined
Accumulated liquid does not revaporise if well is shut in for an extended period
Radial composite model used to analyse well tests. Krg of inner and outer regions determined but transition region not modelled.

SPE 143592

Assessment of Rate-Dependent Skin Factors in Gas Condensate and Volatile Oil Wells

Authors: A.C.Gringarten, O.Ogunrewo, G.Uxukbayev (2011)

Objective of the paper

Determination of a D-Factor in order to calculate rate-dependent skin, when two phases exist in the near-wellbore region.

Methodology used

Multi-rate tests used to determine the total wellbore skin, using single-phase pseudo-pressures and also using two-phase pseudo-pressures.

Conclusions reached

Single-phase pseudo-pressures do not correctly estimate the rate-independent skin and non-Darcy flow coefficients because liquid accumulation around the wellbore adds a further pressure drop in addition to the non-Darcy effect.
Two-phase pseudo-pressures remove the effect of liquid accumulation on the pressure drop, therefore it is possible to calculate a D-Factor using two-phase pseudo-pressures.
The results from theoretical work were matched against field data.